Proceedings of 9th PhD Seminar on Wind Energy in Europe
September 18-20, 2013, Uppsala University Campus Gotland, Sweden

AEROSERVOELASTIC MODELLING AND ACTIVE CONTROL OF VERY LARGE WIND TURBINE BLADES FOR GUST LOAD ALLEVIATION

Bing Feng Ng[1,*], Rafael Palacios [1], J. Michael R. Graham[1], Eric C. Kerrigan[1,2]
[1]Department of Aeronautics, [2]Department of Electrical and Electronic Engineering
Imperial College London, South Kensington Campus, SW7 2AZ
[*]E-mail: b.ng10@imperial.ac.uk

ABSTRACT

The increased flexibility of wind turbine blades necessitates not only accurate predictions of the aeroelastic effects, but also requires active control techniques to overcome potentially damaging loadings and oscillations. An aeroservoelastic model, capturing the structural response and the unsteady aerodynamics of very large rotors, will be used to demonstrate the potential of closed-loop load alleviation using aerodynamic control surfaces.

The structural model is a geometrically-nonlinear composite beam, which is linearised around equilibrium rotating conditions and coupled with a linearised 3D Unsteady Vortex Lattice Method (UVLM) with prescribed helicoidal wake. This provides a direct higher fidelity solution to BEM for the dynamics of deforming rotors in attached flow conditions. The resulting aeroelastic model is in a state-space formulation suitable for control synthesis. Flaps are modeled directly in the UVLM formulation and LQG controllers are finally designed to reduce fatigue by about 26% in the presence of continuous turbulence. Trade-offs between reducing root-bending moments (RBM) and suppressing the negative impacts on torsion due to flap deployment will also be investigated.

NOMENCLATURE

M_η	Discrete mass matrix
C_{gyr}	Gyroscopic damping matrix
K_{gyr}	Gyroscopic stiffness matrix
K_{stif}	Stiffness matrix
Q_{ext}	External forces
η	Nodal dispacements and rotations
ν	Rigid-body velocities
A_c	Influence coefficient matrix
Γ	Vortex circulation strength
w	Aerodynamic downwash
β	Flap deflection angle
δ	External disturbance
n	Time step
t	Time

Sub-, Superscripts

$(\bullet)_0$	Equilibrium conditions
$(\bullet)_b$	Blade representation
$(\bullet)_w$	Wake representation
$(\bullet)_k$	Collocation point representation
$(\bullet)_\beta$	Flap representation
$(\bullet)_\delta$	Gust representation
$\dot{(\bullet)}$	Derivative with respect to time t

Abbreviations

rms	Root-mean-square
DEL	Damage Equivalent load
RBM	Root Bending Moments
UVLM	Unsteady Vortex Lattice Method

INTRODUCTION

The size of wind turbines has been increasing steadily over the years for larger energy capture. Accompanying this is the increased flexibility of blades necessitating accurate aeroelastic predictions, stronger materials and blade-mounted actuators to overcome unnecessary loads and oscillations.

Barlas *et al.* [1,2] documented the most recent developments in the computational modeling of active flaps on wind turbines for load reduction, listing the performance obtained through the use of different control methods. A wide spectrum of predicted performances has been reported with results ranging from 10% up to 30% reduction in loads, depending on the modeling, type of controller, size and distribution of flaps. Among them, the only work that involves aerodynamic modeling using vortex methods is by Riziotis *et al.* [3], who used a vortex panel code coupled with a modal structural module. It was demonstrated through the use of PID control that, under an exponential wind shear profile, a load reduction of up to 30% can be achieved using flaps that range from 15% to 50% span. In fact, most works in active aeroelastic control of wind turbines has relied on classical control methods, such as PD and PID, with only a few of the more recent works considering more advanced techniques, such as LQR or predictive control [2, 4]. This is probably because the intention has normally been to show the potential of feedback control in enhancing the aeroelastic performance of the blades, but in a recent study [5], we have demonstrated that PD required up to 70% more actuation power than a robust controller under similar load reduction targets.

Within this context, this paper will introduce an efficient implementation of the UVLM in state-space representation, which will be coupled to a linearized structural dynamics description of the blade to produce a compact form suitable for aeroservoelastic analysis of wind turbine rotors. The UVLM formulation provides a higher-fidelity solution for the unsteady aerodynamics compared to BEM models, although it is limited to attached flow conditions. This approach will then be used to model the NREL 5-MW reference offshore wind turbine, on which flaps will be attached to demonstrate reduction in root-mean-square (rms) values of RBM, tip deflections and fatigue using LQG controllers. Trade-offs between reducing RBM and suppressing the negative impacts on torsion due to flap deployment will also be investigated.

METHODOLOGY

The aeroservoelastic tool to model the dynamics of large wind turbine rotors is adopted from the integrated framework for the Simulation of High Aspect Ratio Planes (SHARP) [6–9]. SHARP has been extensively verified in previous works for flexible aircraft applications, including static aeroelastic analyses, linear stability analyses, control synthesis and nonlinear open-loop time-marching simulations. In a recent work [10], it has been verified for wind turbine applications. The following description provides an brief overview of the underlying structural and aerodynamic models, which have been tailored in this work for application to large wind turbine dynamics.

Composite beam model

Taking advantage of the slenderness of the blades, the structural deformations is modeled using a composite beam formulation written in a rotating frame of reference [11, 12]. In its original implementation [6], the structural model can account for large static and transient deformations of the blades, which have been reduced to a 1D representation in the 3D space, using an advanced cross-sectional analysis methodology [13]. For the purpose of efficient control synthesis, this work will focus on the linearized equations of motion (EoM) around a possibly geometrically-nonlinear steady-state equilibrium. The incremental form of the beam equation of motion is written as:

$$\begin{aligned} &M_\eta\left(\eta_0\right)\Delta\ddot{\eta}+C_{gyr}\left(\eta_0,\nu_0\right)\Delta\dot{\eta} \\ &+\left[K_{gyr}\left(\eta_0,\nu_0\right)+K_{stif}\left(\eta_0\right)\right]\Delta\eta=\Delta Q_{ext}, \end{aligned} \tag{1}$$

where M_η is the discrete mass matrix, C_{gyr} and K_{gyr} are the gyroscopic damping and stiffness matrices, respectively, and K_{stif} is the stiffness matrix. The nodal displacements and rotations from the finite element discretization is represented by η and external forces are given by Q_{ext}. The hub rigid-body velocity ν is used to prescribe the angular velocity of the rotor.

Unsteady aerodynamics

The aerodynamics are modeled using the discrete-time UVLM [9, 14] with a prescribed helicoidal wake, which allows non-stationary aerodynamics to be captured in low-speed, high-Reynolds-number attached-flow conditions. The UVLM uses vortex rings as fundamental solutions, which are located in lattices that represent the blades and their wakes. The leading segment of the vortex ring is placed along the quarter chord of each panel. The collocation points are then placed at the three-quarter chord, where boundary conditions are imposed.

In the UVLM, Neumann boundary conditions are imposed on the lifting surface. Hence, the normal velocity at each collocation point due to vortices (blade and wake) and motion of the blade has to be zero. This relationship is given by:

$$A_{c,b}\Gamma_b^{n+1}+A_{c,w}\Gamma_w^{n+1}+w^{n+1}=0\,, \tag{2}$$

where Γ_b and Γ_w denotes the circulation at the bound and wake vortex rings, respectively. $A_{c,b}$ and $A_{c,w}$ are the influence coefficients that give the induced velocity normal to blade surface at collocation points (resolved using the Biot-Savart law) due to bound and wake vortices, and n is the time step. The last term w is the downwash at collocation points and is generated by the motion of the lifting surface (mapped from structural beam model), the actuators (such as trailing-edge flaps) and external disturbances (such as gusts). Pressure distribution across each

panel on the lifting surface can subsequently be computed using the unsteady Bernoulli equation [14].

Aeroelastic equations

The continuous-time structural equations of motion are discretized using the Newmark-β method and then coupled with the discrete-time UVLM, providing the full aeroelastic system in discrete-time state-space representation for subsequent control synthesis [8]. The equations can be written in the standard form:

$$\begin{aligned} x^{n+1} &= Ax^n + Bw_\beta^n + Gw_\delta^n, \\ y^n &= Cx^n + Dw_\beta^n + Hw_\delta^n, \end{aligned} \tag{3}$$

where the state vector that completely defines the aeroelastic system is, $x = \left[\Delta\Gamma_b \ \Delta\Gamma_w \ \Delta\eta \ \Delta\dot{\eta}\right]^T$. The control input w_β represents the downwash due to flap motion and the external disturbance w_δ is the downwash due to gust. The output vector, y, includes the desired output (e.g., blade root bending moments, tip deflection).

The inflow speed to the rotor is assumed to be constant and external disturbance enters the system in the form of turbulence (length scale of 250m) in the longitudinal direction that is assumed to be homogeneous in the rotor disk. The turbulence is simulated by passing white Gaussian noise through a filter such that the signal output will have statistical properties same as those under the von Kármán turbulence model [15].

Due to the characteristics of the disturbance, LQG controls will be considered in this paper and closed-loop performance will be measured in terms of the percentage reduction in rms values of RBM and tip deflections and reduction in Damage Equivalent Loads (DEL) [16], while keeping maximum flap deflection angles and rates within the prescribed limits.

NUMERICAL RESULTS

The NREL 5-MW reference wind turbine blade [17] is modeled using the aeroelastic formulation presented above, with the structural beam model clamped on one end to represent the blade. For the aerodynamics, the vortex panels are placed on the outer 85% span of the beam and a helicoidal wake profile is prescribed to enable a linear UVLM representation. The aerodynamics of the inboard segment of the blade with cylindrical cross-section is not modeled here but can be included as additional drag forces.

A flap occupying 20% of the span of the lifting surface and 10% of the local chord is chosen for this study. It is located at a mean position of 80% span. Three operating conditions are considered - 8 m/s, 11 m/s and 14 m/s, which corresponds to regions 2, 2½ and 3 as described in Jonkman *et al* [17] and a TSR of 7.5, 7.0 and 5.5 are chosen, respectively. Turbulence intensities of 6% and 10% are simulated on each operating condition.

TABLE 1: Percentage reduction in RBM and tip deflection for various load cases, using LQG controller with RBM feedback.

Case	Inflow	Turb intensity	rms red. in RBM	rms red. Tip Defl.	DEL red.
1	8 m/s	6%	38%	36%	37%
2	8 m/s	10%	23%	29%	28%
3	11 m/s	6%	23%	30%	29%
4	11 m/s	10%	15%	20%	20%
5	14 m/s	6%	18%	24%	24%
6	14 m/s	10%	12%	16%	17%

For the UVLM, an equal discretization of 10 chordwise, 10 spanwise panels and 20 wake chords is implemented. While a smaller chordwise discretisation was shown to achieve convergence, this discretisation is selected such that the flap will occupy at least one panel. The number of wake chords is determined through a compromise between fidelity and computational cost. In this current configuration, the number of states is already 10,000 for the full rotor. Due to the large size of the model, balanced model reduction is then implemented to obtain reduced order models for controller synthesis [18].

In the following sections, a single rotating blade is first analyzed followed by the full rotor.

Single Rotating Blade

Table 1 shows the percentage rms reduction in RBM and out-of-plane tip deflection for different operating cases, using the LQG controller with RBM feedback for a reasonably long simulation of 200 turbulence length scales. The weights for the LQG controller are tuned separately for each case such that both the flap deflection angle or rate limits of $|\beta| \leq 10^\circ$ and $|\dot{\beta}| \leq 100^\circ$/s are achieved. While the results presented could provide a good estimate of the expected average performances, it will still vary if different disturbance inputs are considered, as turbulence is not bounded.

On average, we are observing around 22% rms reduction in RBM, 26% rms reduction in tip deflection and 26% reduction in DEL for the cases considered in Table 1. For the fatigue analysis, a S-N slope of 10 is selected, typical for composite materials. For all the cases, the limit on the flap deflection angle of $\pm 10^\circ$ is met while the limit on flap deflection rate was less of a concern as it was well below $\pm 100^\circ$/s. For the same inflow speed, lower reductions in RBM and tip deflection were obtained for higher turbulence intensity. As inflow speed is increased, the reduction in RBM and tip deflection is also smaller. This is mainly due

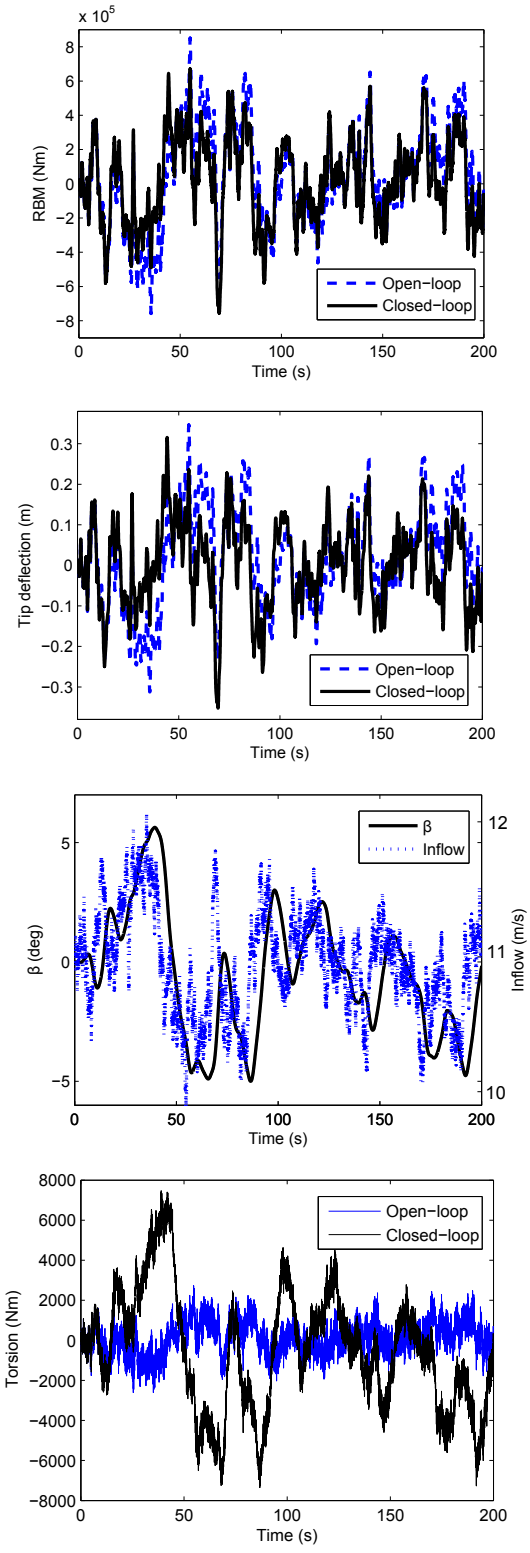

FIGURE 1: Section of the time series for RBM, tip deflection, flap deflection angle, inflow and torsion, with 11 m/s inflow and 6% turbulence intensity (Case 3), using LQG contorller.

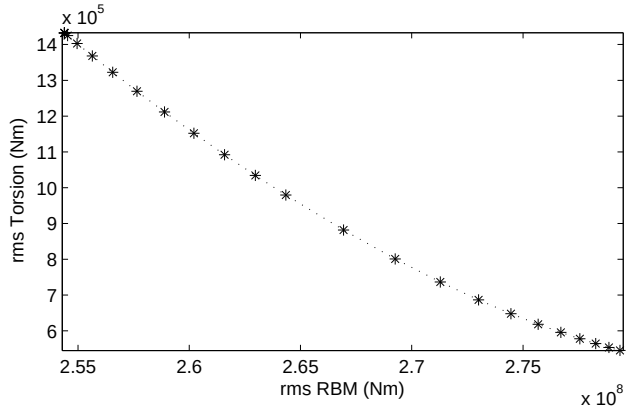

FIGURE 2: Trade-off between RBM and torsion in using active flap controls (Case 4).

to the limit placed on flap deflection angles restricting the performance achievable in higher turbulence intensities and larger inflow speeds. A sample of the time series for the RBM and tip deflections for rated inflow conditions under 6% turbulence intensity is shown in Figure 1, where it is evident that peaks in RBM and tip deflections are suppressed in the closed-loop system. The flap deflection angle β are within prescribed limits. On the same figure, the fluctuation of the inflow is also plotted in which we observe a slight phase lag in the response of the flaps to the inflow turbulence.

While the use of flaps delivers benefits in terms of reducing RBM and tip deflections, it has an adverse effect on torsional forces. As shown in Figure 1, the effects of flap deflection on torsion is significant. As LQG is a Multiple-Input-Multiple-Output (MIMO) controller, torsion can also be included in the objective function to be minimized. Figure 2 shows the trade-off between RBM and torsion in using active flap controls for Case 4. As we move from the left to right in the plot, we are sacrificing reductions in rms of RBM (hence an increase in the value of rms of RBM) for reduced torsional effects. Two observations can be made. Firstly, there is diminishing returns on the reduction in torsion as more RBM is sacrificed. Secondly, if we were to consider the scale of trade-off, we could achieve a larger reduction in Torsion with a given amount of RBM we sacrifice. For instance, a 5% sacrifice in RBM from the leftmost point on the plot is able to achieve close to 50% reduction in torsion.

Full Rotor

The model of the single rotating blade is extended to the full rotor by placing three blades at an azimuth of 120° apart and considering cross influences of bound and wake vortices between the blades as shown in Figure 3. The blades are connected at the hub which we will assume in this analysis to be rigidly clamped.

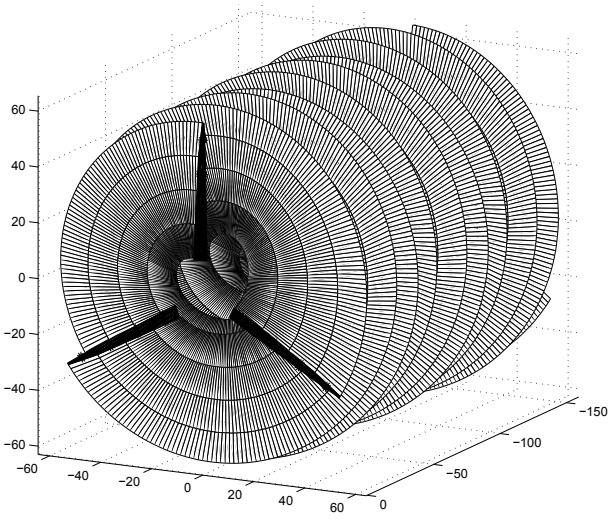

FIGURE 3: Full rotor with wake (3 spanwise, 3 chordwise discretisation and 240 wake chords).

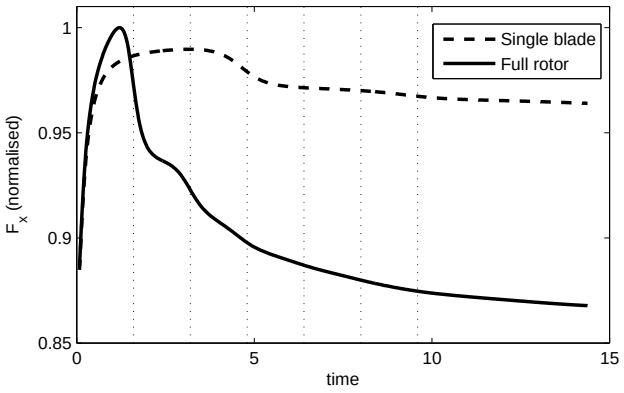

FIGURE 4: Aerodynamic out-of-plane loads for a single rotating blade and for the full rotor. (Vertical dotted lines indicate each time a blade have rotated 120°)

First, we analyse the effect on the aerodynamics loads due to the increased vortex interactions between the three blades. Figure 4 shows the out-of-plane aerodynamic load on one of the blades in the full rotor subject to an impulsive load and the vertical dotted lines indicate each time the blade have rotated 120°. It is evident that in the transient stage, each time the blade passes through the wake shed by another blade or by itself, the aerodynamic loads are reduced. Also plotted on the same figure is a single rotating blade for comparison, showing a slight reduce in load when it passes by its own shed wake after a full rotation. In steady state, the loads in the full rotor configuration is about 15% lower than a single rotating blade.

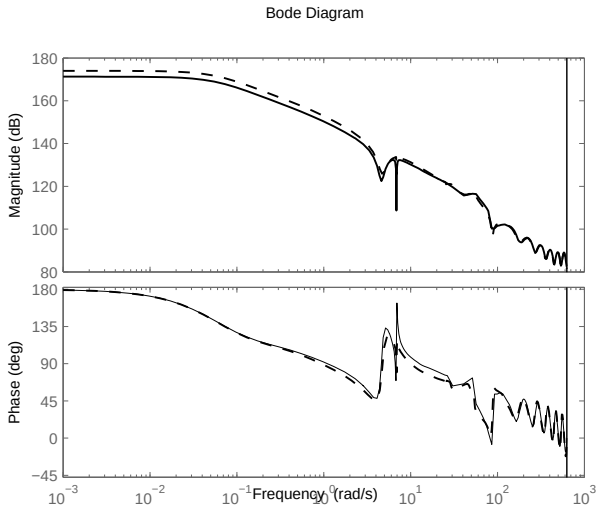

FIGURE 5: Bode plot from w_δ to RBM comparing a single rotating blade (dashed) and the full rotor configuration (solid).

The lower loadings observed in the blades of the full rotor is also evident when analysing the frequency response of the full aeroelastic system. Figure 5 shows the Bode plot from external disturbance w_δ to RBM of a single rotating blade and the full rotor configuration, where we observe slightly smaller gains at low frequencies for the latter.

The closed loop performance is analysed next. For the full rotor configuration and considering the same operating conditions in Case 4, we achieve a slightly higher reduction in RBM and tip deflection of 18% and 21% respectively (against 15% and 20% for single rotating blade in Table 1). As this difference is relatively insignificant, it would be reasonable to conclude that a single rotating blade is sufficient to analyse the load reduction potential of flaps.

CONCLUSIONS

The state-space UVLM formulation coupled with the beam model has been introduced as a model-based design tool for aeroelastic predictions of rotating lifting surfaces and controls. Modeling the 5-MW NREL reference offshore wind turbine blade with trailing-edge flaps using a LQG controller, an average of 22% and 26% rms reduction in RBM and tip deflection is achieved, respectively. The reduction in DEL is around 26%. These results are comparable to existing literature and the flap deflections angles in all cases were within the limits of $\pm 10^\circ$. It also demonstrated the trade-off between RBM and torsion when using a single flap. In the full rotor configuration, lower loadings are observed in the blades, enabling slightly higher closed loop performances compared to a single rotating blade.

ACKNOWLEDGEMENTS

The first author would like to thank the Energy Innovation Programme Office, Singapore, for their funding support, and Dr. Henrik Hesse from Imperial College London, for his invaluable contribution in the structural modeling.

REFERENCES

[1] Barlas, T. K., and van Kuik, G., 2010. "Review of state of the art in smart rotor control research for wind turbines". *Progress in Aerospace Sciences,* ***46***(1), p. 27.

[2] Barlas, T. K., van der Veen, G. J., and van Kuik, G., 2012. "Model predictive control for wind turbines with distributed active flaps: incorporating inflow signals and actuator constraints". *Wind Energy,* ***15***, pp. 757–771.

[3] Riziotis, V. A., and Voutsinas, S., 2008. "Aero-elastic modelling of the active flap concept for load control". In Proceedings of the EWEC.

[4] Wilson, D., Resor, B. R., Berg, D. E., Barlas, T., and van Kuik, G., 2010. "Active aerodynamic blade distributed flap control design procedure for load reduction on the UPWIND 5MW wind turbine". In Proceedings of the 48th AIAA Aerospace Sciences Meeting.

[5] Ng, B. F., Palacios, R., Graham, J.M.R., and Kerrigan, E. C., 2012. "Robust control synthesis for gust load alleviation from large aeroelastic models with relaxation of spatial discretisation". In Proceedings of the EWEA 2012.

[6] Hesse, H., and Palacios, R., 2012. "Consistent structural linearisation in flexible-body dynamics with large rigid-body motion". *Computers & Structures,* ***110-111***(0), pp. 1–14.

[7] Palacios, R., Murua, J., and Cook, R., 2010. "Structural and aerodynamic models in the nonlinear flight dynamics of very flexible aircraft". *AIAA Journal,* ***48***, pp. 2559–2648.

[8] Murua, J., Palacios, R., and Graham, J.M.R., 2012. "Applications of the unsteady vortex-lattice method in aircraft aeroelasticity and flight dynamics". *Progress in Aerospace Sciences*.

[9] Murua, J., Palacios, R., and Graham, J.M.R., 2012. "Assessment of wake-tail interference effects on the dynamics of flexible aircraft". *AIAA Journal,* ***50***, pp. 1575–1585.

[10] Ng, B. F., Hesse, H., Palacios, R., Graham, J.M.R., and Kerrigan, E. C., 2013. "Aeroservoelastic modeling and load alleviation of very large wind turbine blades". In AWEA Windpower.

[11] Simo, J., and Vu-Quoc, L., 1988. "On the dynamics in space of rods undergoing large motions - a geometrically exact approach.". *Computer Methods in Applied Mechanics and Engineering,* ***66***(2), pp. 125–161.

[12] Géradin, M., and Cardona, A., 2001. *Flexible multibody dynamics : a finite element approach*. John Wiley, Chichester ; New York.

[13] Palacios, R., and Cesnik, C., 2005. "Cross-sectional analysis of non-homogeneous anisotropic active slender structures.". *AIAA Journal,* ***43***(12).

[14] Katz, J., and Plotkin, A., 2001. *Low speed aerodynamics*, 2nd ed. Cambridge aerospace series. Cambridge University Press, Cambridge, UK ; New York.

[15] Campbell, C. W., 1986. "Monte carlo turbulence simulation using rational approximations to von Kármán spectra". *AIAA Journal,* ***24***(1).

[16] Freebury, G., and Musial, W., 2000. "Determining equivalent damage loading for full-scale wind turbine blade fatigue tests". In Proceedings of the 19^{th} American Society of Mechanical Engineers Wind Energy Symposium.

[17] Jonkman, J., Butterfield, S., Musial, W., and Scott, G., 2009. Definition of a 5-MW wind turbine for offshore system development. Tech. rep., NREL/TP-500-38060.

[18] Skogestad, S., and Postlethwaite, I., 2005. *Multivariable feedback control : analysis and design*, 2nd ed. John Wiley, Chichester, England ; Hoboken, NJ.